ORIGINAL ARTICLE

Type I CRISPR-Cas targets endogenous genes and regulates virulence to evade mammalian host immunity

Rongpeng Li[1], Lizhu Fang[1], Shirui Tan[1], Min Yu[1, 2], Xuefeng Li[1, 2], Sisi He[1, 2], Yuquan Wei[2], Guoping Li[3], Jianxin Jiang[4], Min Wu[1, 2]

[1]Department of Biomedical Sciences, University of North Dakota, Grand Forks, ND 58203-9061, USA; [2]State Key Laboratory of Biotherapy and Cancer Center, West China Hospital, Sichuan University, and Collaborative Innovation Center for Biotherapy, Chengdu, Sichuan 610041, China; [3]Inflammations & Allergic Diseases Research Unit, Affiliated Hospital of Southwest Medical University, Luzhou, Sichuan 646004, China; [4]State Key Laboratory of Trauma, Burns and Combined Injury, Institute of Surgery Research, Daping Hospital, Third Military Medical University, Chongqing 400042, China

Clustered regularly interspaced short palindromic repeats (CRISPR)-CRISPR-associated (Cas) systems in bacteria and archaea provide adaptive immunity against invading foreign nucleic acids. Previous studies suggest that certain bacteria employ their Type II CRISPR-Cas systems to target their own genes, thus evading host immunity. However, whether other CRISPR-Cas systems have similar functions during bacterial invasion of host cells remains unknown. Here we identify a novel role for Type I CRISPR-Cas systems in evading host defenses in *Pseudomonas aeruginosa* strain UCBPP-PA14. The Type I CRISPR-Cas system of PA14 targets the mRNA of the bacterial quorum-sensing regulator *LasR* to dampen the recognition by toll-like receptor 4, thus diminishing the pro-inflammatory responses of the host in cell and mouse models. Mechanistically, this nuclease-mediated RNA degradation requires a "5′-GGN-3′" recognition motif in the target mRNA, and HD and DExD/H domains in Cas3 of the Type I CRISPR-Cas system. As LasR and Type I CRISPR-Cas systems are ubiquitously present in bacteria, our findings elucidate an important common mechanism underlying bacterial virulence.

Keywords: type I CRISPR; *Pseudomonas aeruginosa*; quorum sensing; LasR; endogenous targeting
Cell Research (2016) **26**:1273-1287. doi:10.1038/cr.2016.135; published online 18 November 2016

Introduction

Clustered regularly interspaced short palindromic repeats (CRISPR) and CRISPR-associated (Cas) systems in bacteria provide adaptive immunity against invading foreign nucleic acids [1, 2]. Currently, the CRISPR-Cas systems are divided into two main classes, 5 types and 16 subtypes, based on the signature in Cas proteins [3, 4]. Previous work revealed that Type II CRISPR-Cas systems, which contain a signature *cas9* gene, also modulate pathogenesis and control bacterial physiology [5]. For example, Cas9 of *Francisella novicida* (*F. novicida*)

targets and degrades endogenous immunostimulatory bacterial lipoprotein (BLP) messenger RNA (mRNA) [6]. As BLP can be directly recognized by the host toll-like receptor 2 (TLR2), its mRNA degradation by Cas9 in *F. novicida* dampens TLR2-mediated host innate immune responses and facilitates bacterial invasion [6]. Meanwhile, Cas9 of *Nesseria meningitidis* and *Campylobacter jejuni* is required for their invasion and replication in epithelial cells, which are essential for bacterial virulence [7]. However, to date, no other CRISPR-Cas family members have been reported to associate with host immune evasion.

Type I CRISPR-Cas systems impact bacterial physiology and virulence. For example, *Pelobacter sp.* encodes an archaeal Type I CRISPR that contains a clustered repeat RNA (crRNA) spacer matching a sequence within the gene encoding a histidyl-tRNA synthetase, and thus has a critical role in bacterial growth defect [8]. *Aggregatibacter actinomycetemcomitans* encodes a crRNA

spacer putatively targeting the glycogen phosphorylase *glgP* to regulate metabolic processes [9]. However, these investigations are limited to bacteria themselves. Thus, it remains unknown whether Class 1 CRISPR-Cas systems (Type I or other types) can regulate bacterial gene expression to impact host defense.

Pseudomonas aeruginosa (*P. aeruginosa*) is a major opportunistic pathogen in the pathogenesis of cystic fibrosis and other immunocompromised diseases [10]. Genomic analysis indicated that the entire family of CRISPR-Cas systems are absent in a well-studied *P. aeruginosa* strain PAO1, whereas Type I-F CRISPR-Cas system is present in a more virulent *P. aeruginosa* strain UCBPP-PA14 (hereafter PA14) [11, 12], and has a role in modulating the production of biofilms [13]. Here, we hypothesized that the Type I-F CRISPR-Cas system in PA14 regulates PA14 virulence to impede host defense. We used wild-type (WT) and total CRISPR-Cas region deletion (ΔTCR) mutant PA14 strains to infect C57BL/6J mice and investigated the role and underlying mechanism of Type I-F CRISPR-Cas system in bacterial infection, particularly in evasion of host defense. Our findings demonstrate that the Type I-F CRISPR-Cas system of PA14 degrades mRNA of the quorum-sensing (QS) master regulator *LasR*, thus allowing the bacteria to evade recognition by host TLR4, and consequently dampening host pro-inflammatory response in both cells and mice. Although Cas9 (Type II CRISPR-Cas, a single member) was reported to be involved in mammalian host defense [6], thus far it remains unclear whether other CRISPR-Cas systems can also subvert host immunity through targeting bacterial endogenous genes. Hence our study has uncovered a novel mechanism employed by bacteria to invade mammalian hosts.

Results

PA14 CRISPR-Cas is necessary for lasR mRNA repression

Although RNA targeting has been reported in both Type II and Type III CRISPR-Cas systems [5], thus far only the Type II CRISPR-Cas system of *F. novicida* was reported to target bacterial endogenous mRNA to alter host immune response during infection [6]. We set out to explore whether additional CRISPR-Cas systems are employed by bacteria to target their endogenous genes in order to alter virulence and impact host immunity. To this end, we first measured transcript levels of *algC*, which controls *P. aeruginosa* LPS synthesis [14], in PA14 WT and total Type I CRISPR-Cas knockout (KO) mutant strain (ΔTCR, including two repeat-rich CRISPR regions and six *cas* genes, Figure 1A and Supplementary

information, Figure S1A) [15]. However, transcript levels of *algC* were similar between these two PA14 strains (Supplementary information, Figure S2A). We then assessed transcript levels of several virulence factors and virulence-associated factors that are known to be injected via the type 3 secretion system (T3SS) into host cells to facilitate invasion [16, 17]. We found that mRNA levels of T3SS exoenzymes ExoT, ExoU and ExoY and virulence-associated factors LasR, LasI, RhlR, RhlI and RpoS were all significantly increased in PA14 ΔTCR mutant compared with those in WT strain, and the increase was reversed in the ΔTCR strain complemented with CRISPR-Cas system (named the complemented strain hereafter; Figure 1B and Supplementary information, Figure S2A). Sequence alignment analysis showed no apparent homology between these virulence factor genes and PA14 CRISPR crRNA spacers except for *lasR* (data not shown). Because the expression of *lasI*, *rhlR*, *rhlI*, *rpoS*, *exoT*, *exoU* and *exoY* is under the control of LasR (Supplementary information, Figure S2B) [18], we hypothesized that the PA14 CRISPR-Cas system modulates virulence by primarily targeting *lasR*.

Plasmid protection assays [19] in PA14 WT and ΔTCR mutant strain were performed to determine whether the PA14 CRISPR-Cas system represses *lasR* expression by targeting chromosomal DNA. WT and ΔTCR mutant P14 strains displayed similar colony forming efficiency upon plasmid p-lasR transformation (Figure 1C), indicating that the PA14 CRISPR-Cas system does not target *lasR* DNA. Exogenous plasmid p-lasR significantly induced *lasR* expression in both PA14 WT and ΔTCR mutant strain, but *lasR* expression level in WT PA14 was much lower than that in the ΔTCR strain (Figure 1D), suggesting that the PA14 CRISPR-Cas can also repress exogenous *lasR* expression. To elucidate whether the PA14 CRISPR-Cas system mediates repression of *lasR* via targeting mRNA for degradation, we treated PA14 strain with rifampicin, an RNA polymerase initiation inhibitor, to prevent mRNA production [20]. We found that *lasR* transcript was rapidly depleted in WT PA14; however, *lasR* transcript depletion was significantly delayed in ΔTCR mutant and restored in the complemented strain (Figure 1E), suggesting that the PA14 CRISPR-Cas system is required for *lasR* mRNA degradation.

Specific PA14 lasR mRNA sequences are targeted by type I CRISPR-Cas systems

To investigate how the PA14 *lasR* transcript level is reduced by CRISPR-Cas system, we examined *lasR* mRNA level in PA14 mutants, each with a deletion of an individual component of the CRISPR-Cas system (Supplementary information, Figure S1B-S1H). Compared
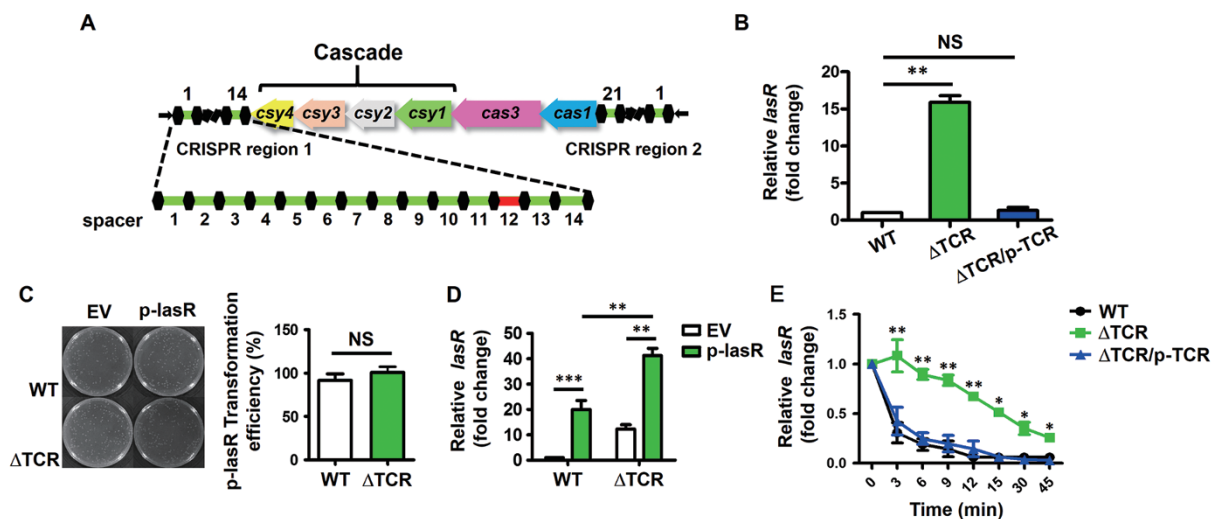
Figure 1 PA14 CRISPR-Cas is necessary for *lasR* mRNA repression. **(A)** Schematic of PA14 CRISPR-Cas locus, comprising Cas protein-coding genes *csy1*, *cas1*, *csy2*, *csy3*, *cas3* and *csy4*, as well as two CRISPR regions (repeats indicated by vertical shadows). **(B)** *lasR* transcripts in PA14 WT, ΔTCR and complemented strains were quantified by qPCR. **(C)** CFU of PA14 WT and ΔTCR mutant strain transformed with *lasR* expressing plasmid p-lasR and empty control plasmid (EV, empty vector), and relative plasmid transformation efficiency was quantified by counting. **(D)** *lasR* transcripts in plasmid-transformed PA14 WT and ΔTCR mutant strains were quantified by qPCR. **(E)** Time course of *lasR* stability in PA14 WT and ΔTCR mutants after treatment with rifampicin. Data are representative of three experiments expressed as means ± SEM (*n* = 3, one-way ANOVA with Tukey's *post hoc*; *$P \leq 0.05$; **$P \leq 0.005$; ***$P \leq 0.001$).

with WT PA14, Δ*csy1*, Δ*csy2*, Δ*csy3*, Δ*csy4*, Δ*cas3* and ΔCR1, but not Δ*cas1* and CR2 mutants, showed significant induction of *lasR* with the highest induction in Δ*cas3* and ΔCR1 mutants (Figure 2A). Furthermore, *lasR* transcript levels in these indicated mutant strains complemented with the corresponding component (Supplementary information, Figure S1B-S1G) were similar to those in WT PA14 (Figure 2A). These data together indicate that Cas3, Csy1-4 and CR1 are primarily involved in the regulation of *lasR* expression.

PA14 CR1 and CR2 contain 14 and 21 crRNA spacers, respectively (Figure 1A). Sequence alignment of each crRNA spacer with *lasR* mRNA sequence showed six potential *lasR* mRNA regions that may be recognized by the PA14 CRISPR-Cas system (Supplementary information, Figure S3B). To identify which regions of *lasR* are actually targeted, we performed *in vitro* cleavage of six 40-nucleotide (nt) RNA substrates, each containing a sequence complementary to a crRNA, by purified Cascade (Csy1-4 complex) and nuclease Cas3 (Supplementary information, Figure S3A-S3B). Cleavage analysis showed that only the *lasR* mRNA region between nt 648 and 687 was significantly cleaved *in vitro* (Supplementary information, Figure S3B).

PA14 CRISPR-Cas system requires a 5′-protospacer, -GG-3′ adjacent motif (PAM) sequence for DNA recog-

nition [21], but sequence for RNA recognition remains unclear. This mRNA locus (648-687 nt) of PA14 has a PAM-like sequence 5′-GGA-3′, followed by nine continuous nucleotides (or 12 across 1 mismatch) hybridized with crRNA1 spacer12 (matured crRNA1-12, Figure 2B). Both Cas3 and crRNA1-12 are required for *in vitro* cleavage, because the RNA substrate was not cleaved in the absence of either Cas3 (Figure 2C) or crRNA1-12 (Figure 2D). In addition, we observed that the WT "5′-GGA-3′"-containing RNA substrate, as well as the last "A mutants" (5′-GGU-3′, 5′-GGG-3′ and 5′-GGC-3′), were cleaved *in vitro*, but when the entire GGA was mutated (5′-UUC-3′), or the first two GG were individually and/or both mutated (5′-GUA-3′, 5′-UGA-3′ and 5′-UUA-3′), cleavage was abolished (Figure 2E). These results indicate that the 5′-GGN-3′ sequence is required for *lasR* mRNA targeting by the PA14 CRISPR-Cas system. We then determined the minimal length of the RNA substrate required for crRNA1-12 binding and found that the first 8 nt downstream of the 5′-GGA-3′ site are required to achieve efficient RNA cleavage *in vitro,* hence termed the core sequence (Figure 2F). We also found that each nt of this core 8-nt sequence is critical for RNA cleavage, as individual mutation of any of the nucleotides resulted in reduced RNA cleavage (Figure 2G).

Figure 2 Analysis of PA14 CRISPR-mediated dynamic RNA degradation. **(A)** *lasR* transcripts in PA14 WT and indicated CRISPR mutant strains were quantified by qPCR. **(B)** Homology comparison between *lasR* mRNA and crRNA1 spacer12 (yellow indicating a PAM-like sequence), and mutation strategy of *lasR* mRNA for 100% hybridization to crRNA1-12. **(C)** Effect of Cas3 concentration on *lasR* mRNA cleavage. **(D)** Effect of crRNA1-12 concentration on *lasR* mRNA cleavage. **(E)** Effect of "5′-GGA-3′" recognition site on *lasR* mRNA cleavage. **(F)** Effects of spacer-matched length on *lasR* mRNA cleavage. **(G)** Effect of gRNA-target RNA mismatch on *lasR* mRNA cleavage. **(H)** Mutation strategy of Cas3 HD, DExD/H and HelC domains. **(I)** *lasR* transcripts in indicated PA14 Cas3 mutant strains were quantified by qPCR. **(J)** Effect of Cas3 catalytic residues on *lasR* mRNA cleavage. **(K)** Binding of Csy1-4 and Cas3 to RNA substrate examined using an EMSA assay. BSA was used as a negative control. Data are representative of three experiments expressed as means ± SEM ($n = 3$, one-way ANOVA with Tukey's *post hoc*; *$P \le 0.05$; **$P \le 0.005$).

The HD and DExD/H domains of Cas3 mediate RNA cleavage

Cas3 contains three major conserved domains: an N-terminal HD-type phosphohydrolase (HD) domain, a central DExD/H helicase (DExD/H) domain with multiple conserved motifs and a C-terminal helicase (HelC) domain [15]. By comparing the amino acid sequences of these three Cas3 domains in *Escherichia coli* UT189, PA2192, *P. mendocina* and *P. stutzeri*, we noticed conserved residues in each domain [15] (also seen in Supplementary information, Figure S4). We generated strains

carrying point mutations at these conserved residues to identify the necessary domains required for repression of *lasR* (Figure 2H). HelC domain point mutants (E825A and R851A) were able to suppress *lasR* transcripts to levels similar to WT PA14, whereas mutants with single-residue substitutions in HD and DExD/H domains (D124A, K427A, D576A and P611A) could not or could only partially retain Cas3 function (Figure 2I). We then performed *in vitro* cleavage assay to examine Cas3 RNA cleavage ability. We found that RNA substrates were cleaved by WT Cas3 and Cas3 HelC domain mutants but

not by Cas3 HD and DExD/H mutants (Figure 2J), clearly indicating the importance of HD and DExD domains in Cas3 RNA cleavage activity. Electrophoretic mobility shift assay (EMSA) produced a similar result: Csy complex and Cas3 HD or DExD/H mutant failed to cleave *lasR* mRNA substrate but retained the ability to bind the substrate, whereas Csy complex plus WT Cas3 or the Cas3 HelC domain mutants cleaved the RNA substrate (Figure 2K), again demonstrating that HD and DExD/H domains are necessary for Cas3 RNase activity.

PA14 CRISPR-Cas deficiency increases PA14 virulence and host innate immune response

To determine the functional role of PA14 CRISPR-Cas in regulation of host immune response, we employed a mouse model to compare differences in host-pathogen interactions between PA14 WT, its CRISPR-Cas deletion mutant and the complemented strains. We intranasally inoculated PA14 WT and the mutant strain to C57BL/6J mice at a multiplicity of infection (MOI) of 5×10^6 colony forming units (CFU)/mouse [22]. Compared with the PA14 WT group, ΔTCR mutant-, Δ*cas3* mutant- and ΔCR1 mutant-infected mice exhibited increased lethality, whereas Δ*lasR* mutant-infected mice showed decreased lethality (Figure 3A), and all these changes in mouse survival could be abolished by complementation of each of the corresponding genes (Figure 3A), suggesting that PA14 CRISPR-Cas system and LasR impact PA14 virulence. Furthermore, although a marked decrease in lethality was observed in ΔTCR mutant-infected mice, ΔTCRΔ*lasR* double mutant-infected mice showed no significant change in lethality compared with Δ*lasR* mutant-infected mice (Figure 3A), suggesting that the PA14 CRISPR-Cas system regulates PA14 virulence primarily
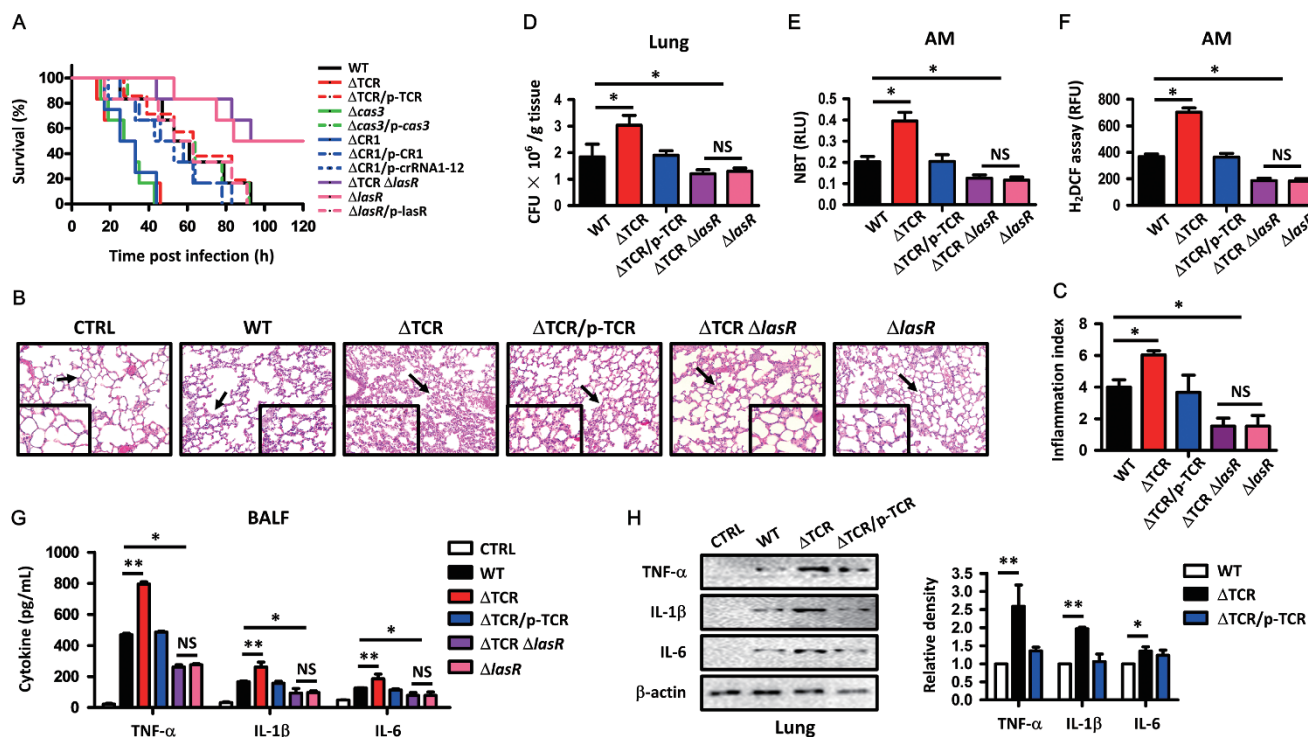
Figure 3 PA14 CRISPR-Cas deficiency increases PA14 virulence and host innate immune response. **(A)** C57BL/6J mice were challenged intranasally with 5×10^6 colony forming units (CFU) of PA14 WT or indicated CRISPR-Cas and *lasR* mutants (*n* = 6, two independent experiments), and survival monitored over time and represented by Kaplan-Meier survival curves. **(B)** Mice were infected with 5×10^6 CFU of PA14 WT, indicated CRISPR or *lasR* mutants per mouse for 24 h. Lung injury and inflammation were assessed by histology. Paraffin-embedded sections were analyzed by H&E staining (arrows indicating the region of insets showing tissue injury and inflammatory influx). Magnification: ×200 (insets: ×400). **(C)** Inflammatory cell infiltration in the lungs was quantified in **B** (10 random areas). **(D)** Bacterial burdens in the lungs after homogenization in PBS. **(E, F)** Superoxide production in AMs was detected by NBT assay **(E)** and H_2DCF assay **(F)**. **(G)** Inflammatory cytokines in BALF were assessed by ELISA. **(H)** Expression of inflammatory cytokines of the lungs was detected by immunoblotting. Data of **D**-**G** are representative of three experiments expressed as means ± SEM (*n* = 3, one-way ANOVA with Tukey's *post hoc*; *$P \leq 0.05$; **$P \leq 0.005$).

through regulating *lasR* expression. Finally, the ΔCR1 mutant complemented with crRNA1-12 showed a similar virulence to PA14 WT or whole CR1-complemented mutant strain (Figure 3A, Supplementary information, Figure S3C and S3D), demonstrating that the PA14 CRISPR-Cas system regulates *lasR* expression using crRNA1-12.

Besides lethality, we examined other mouse phenotypes related to bacterial infection. First, we observed more severe lung injury in ΔTCR mutant-infected mice (Figure 3B). Inflammation index measurements showed a 1.5-fold increase in the lungs of ΔTCR mutant-infected mice versus those of PA14 WT-infected mice (Figure 3C). Bacterial burdens in the lung (Figure 3D), bronchoalveolar lavage fluid (BALF), liver, spleen and kidney all increased significantly in ΔTCR mutant-infected mice (Supplementary information, Figure S5). Both nitroblue tetrazolium (NBT) and dihydro-dichlorofluorescein diacetate (H_2DCF) assays demonstrated that alveolar macrophages (AMs) of ΔTCR mutant-infected mice exhibited an approximate two-fold increase in oxidative stress at 24 h post infection compared with PA14 WT-infected mice (Figure 3E and 3F). To gauge the extent of inflammatory response, we measured secreted pro-inflammatory cytokines in BALF 24 h after PA14 infection by ELISA, as well as the total cytokine levels in mouse lungs by immunoblotting. In BALF of PA14 ΔTCR mutant-infected mice (24 h), levels of TNF-α, IL-1β and IL-6 were significantly elevated compared with PA14 WT-infected mice (Figure 3G). Immunoblotting also showed that the expression levels of these cytokines were higher in ΔTCR mutant-infected mouse lungs (Figure 3H). The lung injury, bacterial burden, oxidative stress and cytokine production in the ΔTCR complemented strain-infected mice were reduced to level similar to that of PA14 WT-infected mice (Figure 3D-3H and Supplementary information, Figure S5), demonstrating that all the phenotypes elicited by the mutants result from the lack of CRISPR-Cas system. In addition, phenotypes in Δ*lasR* mutant- and ΔTCRΔ*lasR* double mutant-infected mice were comparable (Figure 3B-3G and Supplementary information, Figure S5), demonstrating that PA14 CRISPR-Cas system exerts its effect through regulating LasR level.

PA14 CRISPR-Cas deficiency increases bacterial phagocytosis by host alveolar macrophages

To determine the target cell type through which the PA14 CRISPR-Cas system counteracts host immune function, we first analyzed survival at various time points of mouse macrophage cell line MH-S and lung epithelial cell line MLE-12 infected by different PA14 strains. Compared with PA14 WT, survival of MH-S cells decreased significantly following infection by ΔTCR mutant, but was not affected when infected by the complemented strain (Figure 4A). In contrast, survival of MLE-12 cells was not significantly decreased following infection by ΔTCR mutant (Figure 4B), suggesting that macrophages may be the active innate immunity cells involved in this model. The production of TNF-α, IL-1β and IL-6 cytokines was markedly elevated in MH-S cells infected by ΔTCR mutant, but not in cells infected by the complemented strain, again indicating that the PA14 CRISPR-Cas system modulates host inflammatory responses (Figure 4C and 4D). Confocal laser scanning microscopy (CLSM) showed significant colocalization of EGFP-tagged ΔTCR mutant with RFP-tagged Rab5, a marker of phagosome/early endosome, in MH-S cells (Figure 4E). Quantification of CLSM result showed that number of bacteria phagocytized by MH-S cells, and number of Rab5 puncta increased after TCR mutant infection (Figure 4F and 4G), suggesting that PA14 CRISPR-Cas deficiency may be associated with an increase in bacterial phagocytosis in AMs.

PA14 CRISPR-Cas regulates innate immunity through TLR4-related signaling

Inflammatory responses are critical for host defense and bacterial clearance [23]. To uncover the signaling pathway that the PA14 CRISPR-Cas system modulates and thereby impacts on host inflammatory responses, we analyzed transcript profiles of immune regulatory factors in MH-S cells using an innate and adaptive immune response array-based quantitative real-time polymerase chain reaction (qPCR) assay (Figure 5A). We observed a much higher production of inflammatory response factors and its mediators including cytokines, chemokines and proteins involved in antibacterial defense (Supplementary information, Table S1). In addition, the expression of key components of two critical signaling pathways, the TLR4/NF-κB pathway and Jak2/Stat6 pathway [24, 25], was upregulated more than 10 fold in ΔTCR mutant-infected MH-S cells compared with PA14 WT-infected cells (Figure 5A). To validate the results of transcript profiling, we measured the levels of TLR2, TLR4, Jak2, NF-κB, Stat6, phosphorylated Jak2 (p-Jak2), p-NF-κB and p-Stat6 in MH-S cells 30 min post infection of PA14 ΔTCR mutant and WT by immunoblotting. We found that levels of these proteins were much higher in mutant-infected cells than in PA14 WT-infected cells (Figure 5B). We further explored the effect of the PA14 CRISPR-Cas system on TLR4 expression and p-NF-κB nuclear translocation in MH-S cells [26]. CLSM analysis showed that TLR4 was rapidly induced (Figure 5D), and
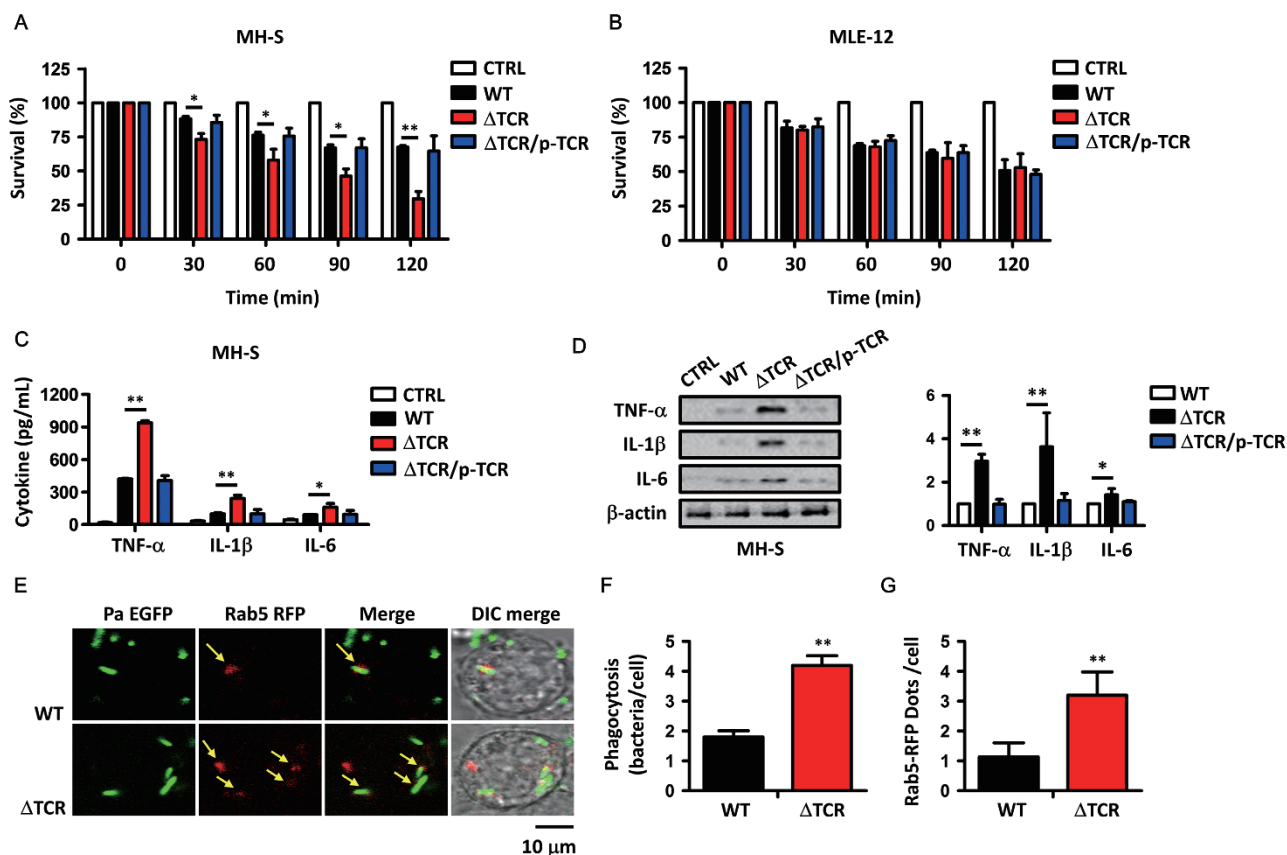
Figure 4 PA14 CRISPR-Cas deficiency increases bacterial phagocytosis by host alveolar macrophages. **(A**, **B)** MH-S and MLE-12 cells were infected with PA14 WT, ΔTCR and complemented strains at an MOI of 20:1 for 2 h. Time course of survival was determined by an MTT assay. **(C)** Inflammatory cytokines in medium were assessed by ELISA. **(D)** Expression of inflammatory cytokines in MH-S cells was detected by immunoblotting. **(E**-**G)** MH-S cells were transfected with Rab5-RFP (red) for 24 h, and then were challenged with PA14 WT and ΔTCR mutant, both harboring a plasmid pMQ70-EGFP, at an MOI of 20:1 for 30 min. Colocalization (arrows) of bacteria and Rab5 observed by confocal laser scanning microscopy (CSLM). **(E)** Uptake of the bacteria **(F)** and Rab5 dots **(G)** were quantified (random 100 cells). Data are representative of three experiments expressed as means ± SEM (n = 3, one-way ANOVA with Tukey's *post hoc*; *P ≤ 0.05; **P ≤ 0.005).

p-NF-κB was also quickly activated and translocated into the nucleus (Figure 5C) in ΔTCR mutant-infected MH-S cells, compared with PA14 WT-infected cells. All these effects were abolished when the complemented strain was used (Figure 5B-5D). To determine whether LasR deficiency in PA14 dampens host inflammatory responses, we attempted to compare the host immune response in Δ*lasR* mutant- and PA14 WT-infected mice. Secretion and expression of TNF-α, IL-1β and IL-6 in Δ*lasR* mutant-infected mouse lungs were decreased compared with PA14 WT-infected mice and similar decrease was observed in NH-S cells (Supplementary information, Figure S6A and S6B). Similarly, expression levels of TLR-4, NF-κB and p-NF-κB were also decreased (Supplementary information, Figure S6C). In addition, deficiency of LasR in PA14 also reduced the phagocytosis of

macrophages (Supplementary information, Figure S6D). These data collectively demonstrate that LasR is required for establishing immune response in host macrophages. In addition, AMs isolated from human BALF upon infection with PA14 WT, ΔTCR mutant and Δ*lasR* mutant behaved similarly to mouse macrophages (Supplementary information, Figure S7). These findings suggest that the PA14 Type I CRISPR-Cas system may modulate immune responses in human macrophages through targeting *lasR* mRNA.

To determine whether TLR4 mediates the inflammatory response that is targeted by PA14 CRISPR-Cas system, we compared cytokine production in primary AMs of WT or TLR4 KO mice (Figure 5E) after PA14 infection. In WT mice, ΔTCR mutant infection increased TNF-α, IL-1β and IL-6 secretion by two-fold on average
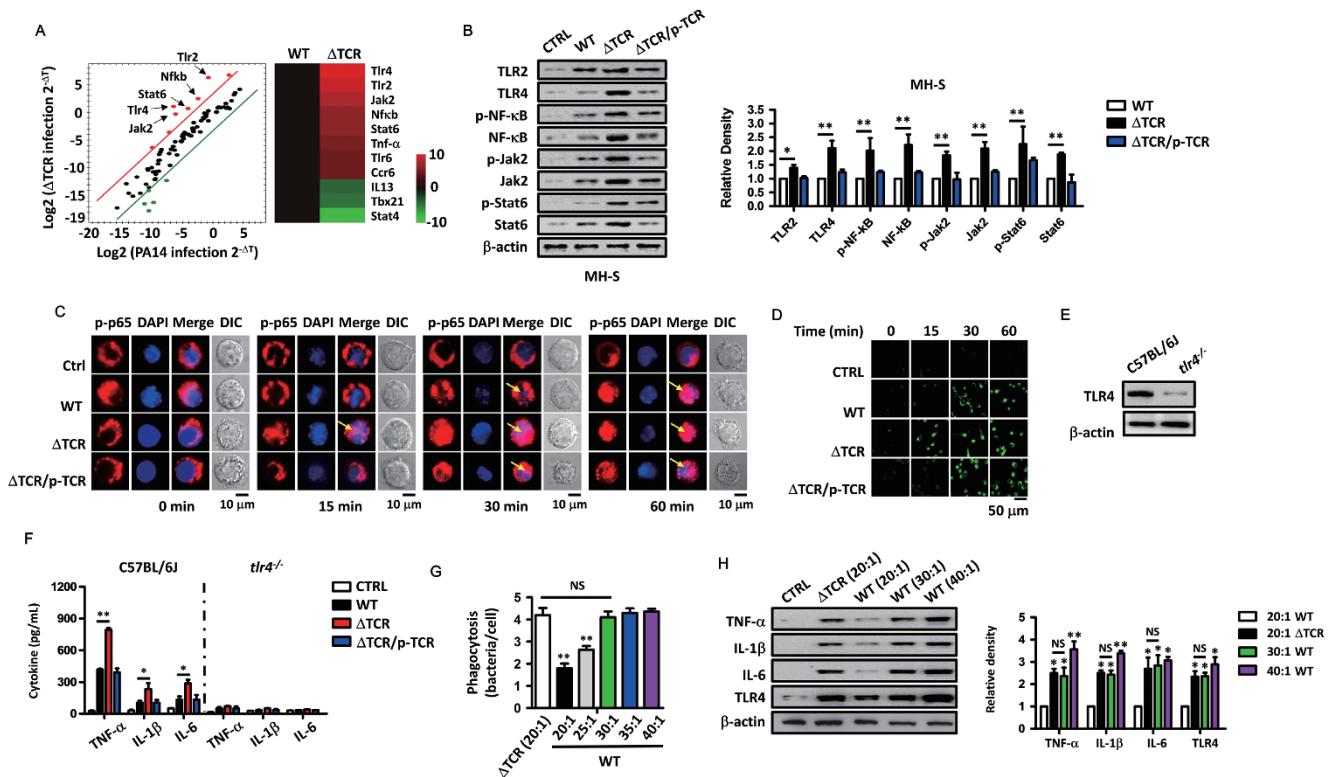
Figure 5 PA14 CRISPR-Cas regulates innate immunity through TLR4/NF-κB signaling. **(A)** MH-S cells were infected with PA14 WT and ΔTCR mutant at an MOI of 20:1 for 2 h. qPCR primer assay of immune response-related factors in ΔTCR mutant-infected MH-S cells versus PA14 WT-infected controls. Red dots indicate increased genes and green dots indicate decreased genes (over 10-fold change and *P* ≤ 0.05, *n* = 2 biological replicates). **(B)** Expression of TLR2, TLR4 and indicated signaling factors in PA14 WT-, ΔTCR mutant- and complemented strain-infected MH-S cells (30 min). **(C)** MH-S cells were infected with PA14 WT, ΔTCR mutant and complemented strain at an MOI of 20:1 for 0, 15, 30 and 60 min. CSLM results show the translocation of p-NF-κB (p-p65) in MH-S cells using immune staining. DAPI was used for staining the nucleus (arrows showing the nuclear translocation). **(D)** CSLM results show the production of TLR4 in MH-S cells. **(E)** TLR4 expression was determined in C57BL/6J WT and TLR4 KO mice by immunoblotting. **(F)** Secretion of TNF-α, IL-1β and IL-6 in BALF from C57BL/6J WT and TLR4 KO mice after WT PA14, ΔTCR mutant and complemented strain infection. **(G)** Phagocytosis of indicated MH-S cells was measured by CFU count assay. MH-S cells were infected with an MOI of 20:1, 25:1, 30:1, 35:1 and 40:1 PA14 WT. The MOI of 20:1 ΔTCR mutant infection was a control. **(H)** Expression of TLR4 and production of TNF-α, IL-1β and IL-6 in PA14 WT-infected and ΔTCR mutant-infected MH-S cells were detected by immunoblotting. Data are representative of three experiments expressed as means SEM (*n* = 3, one-way ANOVA with Tukey's *post hoc*; *P* ≤ 0.05; **P* ≤ 0.005).

in AMs compared with the infection of the complemented strain and PA14 WT infection (Figure 5F). However, levels of TNF-α, IL-1β and IL-6 were diminished following infection with any of the PA14 strains in TLR4 KO mice (Figure 5F), suggesting that CRISPR-Cas-modulated inflammatory response is dependent on TLR4.

Our above results suggest a role of PA14 Type I CRISPR-Cas system in regulating phagocytosis and immune response of host macrophages. We next investigated the impact of phagocytosis on CRISPR-Cas-modulated inflammatory responses. We first determined the ratio of bacteria to host cells that could cause the same phagocytosis rate for PA14 WT and ΔTCR mutant strains, and

found that 30:1 of PA14 WT induced the same phagocytosis level in MH-S cells as that induced by 20:1 of ΔTCR mutant (Figure 5G). At the same phagocytosis level, we observed no apparent difference in the expression levels of TLR4, TNF-α, IL-1β and IL-6 between ΔTCR mutant-infected cells and PA14 WT-infected cells (Figure 5H). These data indicate that while PA14 CRISPR-Cas system may modulate both pro-inflammatory response and phagocytosis, phagocytosis itself may also impact pro-inflammatory response in macrophages (Figure 6G).

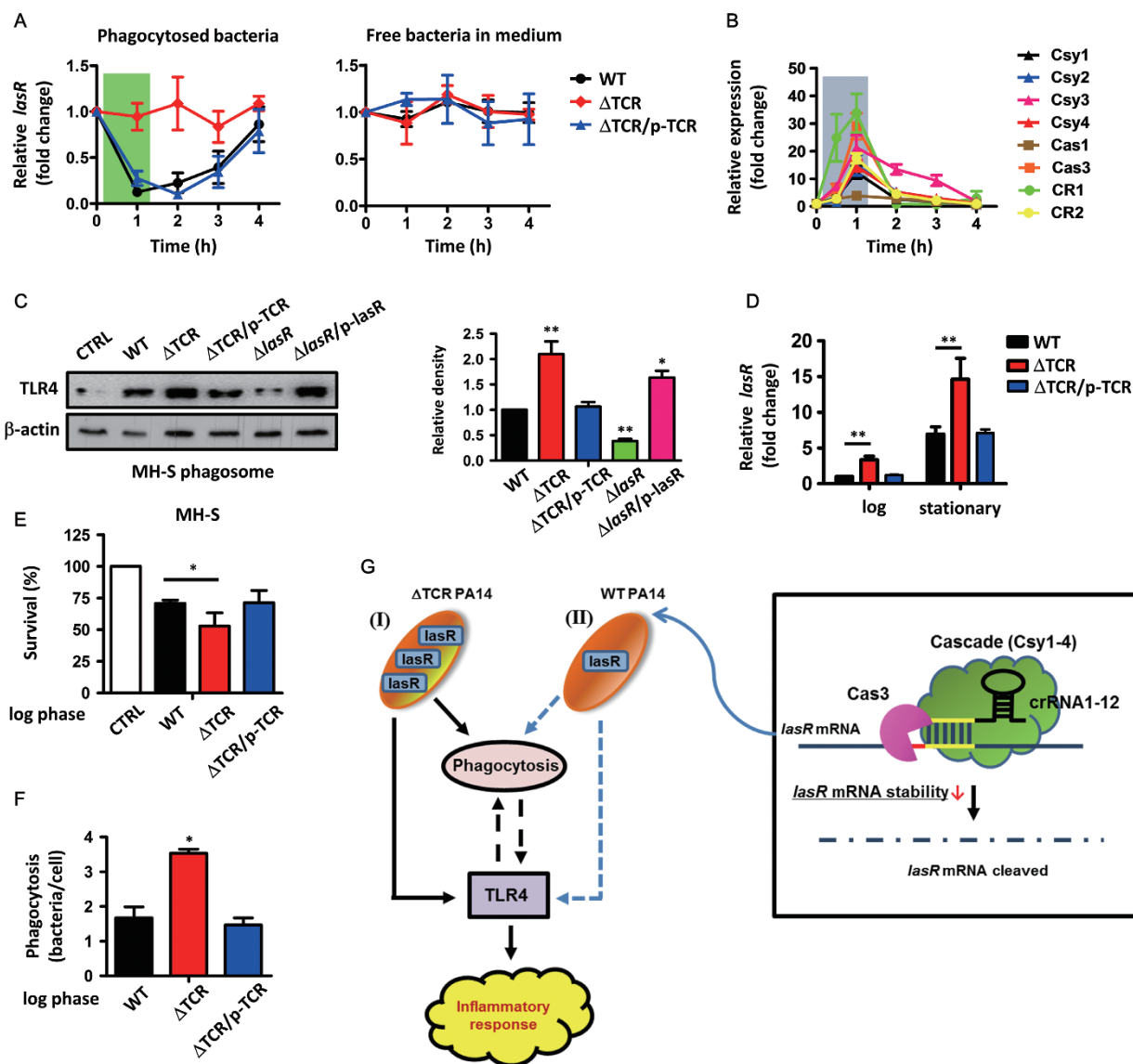*PA14 CRISPR-Cas modulates TLR4 signaling by tempo-*

Figure 6 PA14 CRISPR-Cas modulates TLR4 signaling by temporal repression of *lasR*. **(A)** *lasR* transcripts in invading bacteria were quantified by qPCR. MH-S cells were infected with PA14 WT, ΔTCR mutant and the complemented strain at an MOI of 20:1. Bacteria in the medium or in the phagosome of MH-S cells were collected at 0, 1, 2, 3 and 4 h after infection. **(B)** Time course of transcripts of PA14 CRISPR-Cas components in MH-S cells that have phagocytized PA14 WT strain. **(C)** TLR4 expression in PA14 WT-, ΔTCR mutant-, Δ*lasR* mutant- and the complemented strain-infected MH-S phagosomes, determined by immunoblotting. **(D)** Transcripts of *lasR* in PA14 WT and mutants were quantified by qPCR. RNA was isolated when PA14 WT, ΔTCR and the complemented strains grew at an $OD_{600\ nm}$ of 0.5 (log phase) or 2.0 (stationary phase) in M9 medium. **(E, F)** MH-S cells were infected with PA14 WT, ΔTCR mutant and the complemented strain in log phase at an MOI of 20:1 for 2 h. Survival rates were determined by an MTT assay **(E)**, and phagocytosis of indicated MH-S cells were measured by CFU count assay **(F)**. Data are representative of three experiments expressed as means ± SEM (n = 3, one-way ANOVA with Tukey's *post hoc*; *$P \leq 0.05$; **$P \leq 0.005$). **(G)** Model of PA14 evasion from macrophages mediated by function of the CRISPR-Cas system to target *lasR* mRNA: (I) PA14 lacking the CRISPR-Cas system (P14 ΔTCR): when captured in phagosome, the LasR-dependent virulence factors of PA14 activate host TLR4 expression, leading to elevated inflammatory responses. (II) WT P14: once entering the phagosome, the expression of CRISPR-Cas components of PA14 is upregulated. The crRNA1-12 structure is associated with Cascade (Csy1-4 complex) and interacts with *lasR* mRNA through a sequence matching part of crRNA1-12 (yellow; PAM like sequence, red). *lasR* mRNA is then cleaved by Cas3, leading to its degradation. Reduction in *lasR* levels decreases TLR4 expression and TLR4-mediated recognition in macrophages, thus dampening host inflammatory responses. It is also likely that such decrease in TLR4 expression levels may in turn lead to suppressed phagocytosis, which could further compromise the immune response. The exact mechanism by which LasR of P14 regulates host phagocytosis remains undefined.

ral repression of lasR

To determine whether activation of the CRISPR-Cas system and repression of *lasR* is an active evasion mechanism, we analyzed *lasR* transcript levels in phagosomes of MH-S cells following PA14 WT, ΔTCR mutant and the complemented strain infection. *lasR* transcripts of phagocytized PA14 WT and ΔTCR complemented strain in MH-S cells were initially decreased and then slightly increased, whereas *lasR* transcript levels in phagocytized ΔTCR mutant did not change significantly during 4 h infection (Figure 6A). In contrast, *lasR* transcript levels of all the PA14 strains in the medium remained constant (Figure 6A) during the entire infection process. Similarly, all the CRISPR-Cas components of phagocytized PA14 WT (*csy1-4, cas1, cas3,* CR1 and CR2) showed a rapid induction during PA14 WT infection (Figure 6B). We examined TLR4 levels in phagosomes and found that TLR4 expression was significantly increased in PA14 ΔTCR mutant-infected MH-S cells, but markedly decreased in PA14 Δ*lasR* mutant-infected MH-S cells compared with PA14 WT-infected cells (Figure 6C). These data collectively suggest bacteria evade from TLR4 recognition by a rapid activation of CRISPR-Cas system and repression of *lasR* mRNA production.

As LasR is the critical QS regulator [27], we compared the QS phenomenon between PA14 WT and the mutants. Both biofilm formation and pyocyanin production, two best known QS phenomena in *P. aeruginosa* [27], were not significantly changed when the CRISPR-Cas system was deleted (Supplementary information, Figure S8), suggesting that CRISPR-Cas system does not impact on host inflammatory responses through modulating the regulatory activity of LasR in QS. As all of the above-mentioned data were collected using bacteria from stationary phase (OD_{600} ~2.0), we repeated certain key experiments using the OD_{600} ~0.5 cultures (log phase) of PA14 strains (Figure 6D-6F). Similar to those of bacteria in stationary phases, PA14 ΔTCR mutant culture in the log phase also had an increased level of *lasR* transcript, and the level returned to normal when ΔTCR was complemented by p-TCR (Figure 6D). The log phase PA14 ΔTCR mutant also showed increased virulence to MH-S cells (Figure 6E), and had increased uptake in MH-S cells (Figure 6F). These data suggest that our proposed evasion mechanism also applies at the early log phase.

Discussion

This study reports that the Type I-F CRISPR-Cas system of PA14 has a non-canonical function in altering its own virulence by targeting and repressing LasR, enabling an evasion from the host defense and leading to a reduced cytokine production and impaired immune response. Thus endogenous targeting by CRISPR-Cas systems may benefit bacterial invasion and survival in the host. Bacterial endogenous RNA targeting is mostly reported in the Type III CRISPR-Cas system [28], and several examples have been presented in Type II CRISPR-Cas system [6, 7, 29]. However, RNA targeting in the Type I CRISPR-Cas system has thus far not been investigated.

Using an established mouse infection model, we demonstrate that CRISPR-Cas deficiency increases PA14 virulence and results in severe lung injury and increased mortality in mice, due to an excessive inflammatory response activated mainly through TLR4-related signaling. We identify a role for Type I CRISPR-Cas proteins of PA14 in modulating the expression of endogenous QS regulator LasR and evading the recognition of host TLR4, thereby significantly reducing inflammatory responses (Figure 6G). Mechanistically, the PA14 CRISPR-Cas system recognizes and cleaves *lasR* mRNA, which contains a "5′-GGA-3′" recognition site and core 8 nts matching the crRNA1-12 sequence, in a manner depending on HD and DExD domains in Cas3.

lasR mRNA contains several potential target sites based on bioinformatic analysis, and *in vitro* RNA cleavage assay confirmed that the nt 648-687 region of *lasR* mRNA loci is the predominant target site. Though this site does not match crRNA1 spacer12 optimally, the efficiency of *lasR* cleavage is robust (Figure 2). This is similar to the capacity of the PA14 CRISPR-Cas system targeting bacteriophage DSM3, which uses a crRNA that does not 100% match the prophage gene in the genome [13]. Consistent with this, *F. novicida* Cas9 targeting of BLP mRNA does not require a perfect match for gene targeting [6]. Further experiments in our study have revealed many other features of bona fide *lasR* target site (Figure 2), including (1) a "5′-GGA-3′" sequence is required for recognition with the first two "G" being specifically crucial; (2) at least eight continuous nts next to the "5′-GGA-3′" site are required for hybridizing with crRNA1-12; (3) each of the 8 nts is required for successful cleavage. The "5′-GGN-3′" PAM site has been previously demonstrated for recognition and cleavage of DNA targets for adaptive immunity targeting phage genomes in *P. aeruginosa* CRISPR [21]. Here we for the first time demonstrate that this "5′-GGN-3′" sequence may also be required for RNA targeting.

Studies have revealed that among Cas proteins in Type I CRISPR-Cas systems, Cas3 has as a key role in programing gene expression [30] by acting as a single-strand DNA nuclease and ATP-dependent helicase [31]. Csy1-4 proteins constitute the cascade [32], wherein Csy4 func-

tions in processing crRNA transcripts, whereas Csy1-3 proteins are required to stabilize the crRNA produced by Csy4 [32]. On the other hand, Cas1 is not required for this procedure, but has a role in acquiring new spacers [33]. Our results are consistent with these studies, as qPCR data showed that Cas3 and Csy1-4 proteins, but not Cas1, are involved in the regulation of *lasR* transcript levels. In addition, we found that Cas3 HD and DexD/H domains are required for its RNase activity to cleave *lasR* mRNA.

Our data have established that the PA14 CRISPR-Cas system regulates host immune response by suppressing phagocytosis and inhibiting TLR-4-related signaling in macrophages. *F. novicida* Type II CRISPR-Cas system also regulates host inflammatory responses in host macrophages, but with notable differences that *F. novicida* Cas9 does not regulate bacteria's uptake by macrophages and *F. novicida* Cas9 impacts on immune response mediated by the IL-6/TLR2 signaling pathway [6, 34]. During *P. aeruginosa* infection, early inflammatory signaling following NF-κB activation is dependent on both TLR2 and TLR4 [35], but here the inflammatory response permitted by the PA14 CRISPR-Cas-deletion mutant was primarily TLR4-dependent. Our data show that increased bacterial uptake affects inflammatory responses in host AMs (Figure 5), suggesting that manipulation of bacterial uptake may modulate host immunity during clinical infection. The detailed interesting mechanism by which phagocytosis impacts inflammatory responses requires further investigation.

The process by which PA14 uses CRISPR-Cas system to evade macrophage recognition is a dynamic. All CRISPR-Cas components were temporally induced when PA14 was localized to the phagosome inside AMs, and this coincided with a reduction of *lasR* expression (Figure 6). In the absence of CRISPR-Cas systems, the repression of *lasR* in PA14 was significantly reduced and delayed, whereas the recruitment and/or expression of TLR4 into the phagosome of AMs was enhanced (Figure 6). These data collectively illustrate a role for the PA14 CRISPR-Cas system during intracellular infection, allowing temporal repression of *lasR* when PA14 is in the proximity of TLR4 in the phagosome, thus facilitating the evasion of innate immunity. Consistent with our findings, a similar evasion role was reported in *F. novicida* [6]. Although BLPs in *F. novicida* can be directly recognized by TLR2, the particular *lasR*-related virulence factor mediating TLR4 recognition in the host remains unclear. It was reported that ExoS of *P. aeruginosa* strain PAO1 can be recognized by TLR4 during infection [36]. PA14 does not have ExoS, but its ExoT is 70.9% homologous to PAO1 ExoS amino acid sequence. It is conceivable that

PA14 ExoT may also be recognized by TLR4. Alternatively, PA14 CRISPR-Cas may influence TLR4 expression as it is enhanced following the infection of PA14 CRISPR-Cas-deficient mutant. Both hypotheses warrant further investigation.

To date, CRISPR-Cas systems have been found in 39% of sequenced bacterial and 88% of archaeal genomes [37]. In common pathogenic bacteria, CRISPR-Cas Type I systems are more prevalent, covering 70% of species [38]. In addition, self-targeting crRNAs have been predicted to target genes encoding hypothetical proteins in pathogens *Clostridium botulinum* and *Yersinia pestis*, two sporulation genes and a gene involved in S-layer biosynthesis in *C. tetani*, and *fdrA* gene involved in protein transport in *Enterobacter sp.* [39]. These findings suggest that our newly described regulatory mechanism may be adopted by other organisms when interacting with eukaryotic cells. To confirm this notion, we successfully detected temporal activation of CRISPR-Cas transcripts in two other Gram-negative bacteria, *Klebsiella pneumoniae* NTUH-K2044 [40] and *E. coli* K12 [41] during infection in MH-S cells, which exhibited immune response patterns similar to those seen in PA14 infection (Supplementary information, Figure S9). Among the indicated pathogens listed in Supplementary information, Table S2, 24 have Type I CRISPR-Cas systems and 21 have QS systems. It is interesting to note that 13 of these bacteria contain both Type I CRISPR-Cas and QS systems, similar to PA14, suggesting that the self-targeting role for CRISPR-Cas described in this study may also exist in those organisms. Our results and those from Weiss's and colleagues [6] substantiate endogenous mRNA targeting by the CRISPR-Cas system as a common mechanism to evade host immune responses. These findings extend the hypothesis that CRISPR-Cas systems can reshape bacterial virulence to effectively escape mammalian immune defense. This concept may also have strong implications for the development of effective therapy, where the pace of pharmacological innovation struggles to keep up with rapidly growing antibiotic resistance in a variety of superbugs.

Materials and Methods

Mice

Female C57BL/6J mice were obtained from the Jackson Laboratory [42], and *tlr4*$^{-/-}$ mice in C57BL/6J background (originally from S Akira, Osaka University, Osaka, Japan) were kindly provided by Dr Jyotika Sharma (University of North Dakota). Mice were kept in a pathogen-free facility at the University of North Dakota. All animal studies were approved by the University of North Dakota Institutional Animal Care and Use Committee and performed in accordance with the animal care and institutional

guidelines (IACUC approval #1204-4). The animal experimental procedures including treatment, care and endpoint choice, followed Animal Research: Reporting *In Vivo* Experiment guidelines.

Primary cells and cell lines

Primary AMs were obtained from BALF. Mice were killed, and the thoracic cavity and the trachea were dissected. A small incision was made in the trachea via a 1-ml syringe with an angiocath (BD Biosciences, Franklin Lakes, NJ). Mouse lungs were lavaged three times with 1 ml PBS containing 1% FBS (Fisher Scientific, Pittsburgh, PA). The retained BALF was centrifuged at $600 \times g$ for 5 min at 4 °C. Cell pellets were resuspended in RPMI 1640 (Fisher Scientific) supplemented with 10% FBS and incubated on culture plate for 1 h at 37 °C/5% CO_2 incubator to allow attachment of macrophages. Non-adherent cells were removed by washing with normal saline. Murine MLE-12 lung type II epithelial cells and MH-S AMs cells were obtained from American Type Culture Collection (Manassas, VA) and cultured following the manufacturer's instructions [42]. Human primary AMs from BALF samples were obtained through assistance by Dr Arvind Bansal at Altru Hospital. All experiments with human AMs were approved by the University of North Dakota Institutional Review Board Committee (IRB-200908-036, exempt 5) and have been conducted according to the principles expressed in the Declaration of Helsinki.

Bacterial preparation and infection experiments

The *P. aeruginosa* strain PA14 and its CRISPR-Cas component mutants, complementary strains were kindly provided by Dr George A O'Toole (Dartmouth Medical School) [15]. Other PA14 mutant strains were constructed in this study (Supplementary information, Table S3). *K. pneumonia* NTUH-2044 was provided by Dr Jingtang Wang (National Taiwan University, China). *E. coli* K12 was ordered from New England BioLabs (Ipswich, MA). WT PA14 and indicated mutants were also incubated in minimum synthetic M9 medium consisting of 48 mM Na_2HPO_4, 22 mM KH_2PO_4, 9 mM NaCl, 19 mM NH_4Cl, 2 mM $MgSO_4$, 100 mM $CaCl_2$ and 10 mM glucose at pH 7.2. Medium for PA14 mutants containing pMQ70 series vectors was supplemented with 2 mg/ml carbenicillin.

Bacteria were generally grown for about 16 h (OD_{600} ~2.0, stationary phase) in LB medium consisting of 1% w/v tryptone, 0.5% w/v yeast extract and 1% w/v NaCl at 37 °C. In certain indicated cases, bacteria were grown for about 3 h (OD_{600} ~0.5, log phase). Various mammalian primary cells or cell lines were changed to antibiotic-free medium and challenged by bacteria in an MOI of 20:1 bacterium-cell ratio (some cases using other MOI). Mice were sedated with 40 mg/kg ketamine and then intranasally inoculated with 5×10^6 CFU/mouse of bacteria in 50 µl PBS as described [22]. Mice were monitored for symptoms and killed when they were moribund.

Plasmid construction

For complementation, WT and mutated *cas3* genes were amplified from PA14 genomic DNA with specific primers by overlap PCR (single residue mutant sequences were introduced in primers, Supplementary information, Table S3) and subcloned into the *Eco*RI and *Hind*III sites of pMQ70 vector. *lasR* gene and total CRISPR-Cas region were also amplified from PA14 genomic DNA and cloned into the *Hind*III and *Bam*HI sites of pAK1900 vector. Total

CR1 region and crRNA1-12 were cloned into the *Eco*RI and *Xho*I sites of pgRNA vector. For EGFP labeling, *egfp* gene was amplified from pEGFP vector (Clontech, Mountain View, CA) and subcloned into the pMQ70 vector using the same endonuclease sites. For *lasR* gene KO, 500 bp up and downstream of *lasR* gene were amplified and cloned into the *Sac*I and *Xba*I sites of pCVD442 vector. Constructed plasmids were electroporated into WT PA14 or indicated mutants using an Electroporator 2510 system (settings: 25 µF, 200 Ω, 2.5 kV; Eppendorf, Hauppauge, NY). Transformants were selected and maintained in LB medium containing 2 mg/ml of ampicillin. All enzymes used in molecular cloning were purchased from New England Biolabs.

RNA isolation and qPCR

RNA was isolated from bacterial cultures or infected macrophages at the indicated time points. A 50-ng DNA-free RNA was used for the first strand of cDNA synthesis using a SuperScript III first-strand synthesis system (Fisher Scientific). qPCR was performed using the iTag Universal SYBR Green Supermix (Bio-Rad, Hercules, CA) and gene-specific primers (Supplementary information, Table S3, synthesized in Integrated DNA Technologies, Coralville, IA), in a CFX Connect Real-time PCR Detection System (Bio-Rad). The separate well $2^{-\Delta\Delta C_T}$ cycle threshold method was used to determine relative quantitative levels of individual gene [22]. For bacteria, relative transcript levels were normalized to 16S rRNA, whereas in mammalian cell, relative transcript levels were normalized to GAPDH.

Histological analysis

Lung sections were fixed in 4% formalin for 24 h and then processed to hematoxylin and eosin staining in AML Laboratories (Baltimore, MD), and observed using Nikon 80i Eclipse (upright) microscope [22]. The degree of cellular infiltration was scored using previously described methods [43]. The index was calculated by multiplying severity by extent in 10 random areas, with a maximum passible score of 9 [44].

Bacterial burden assay

AMs from BALF and lung, spleen, liver and kidney tissues, were homogenized with PBS and spread on LB dishes to enumerate bacterial numbers. The dishes were cultured in a 37 °C incubator overnight, and colonies were counted. Triplicates were done for each sample and control [22].

Nitroblue tetrazolium assay

AMs from BALF were grown in a 96-well plate in serum-containing medium at 37 °C for 4 h and NBT (1 µg/ml) dye (Sigma-Aldrich, St Louis, MO) into each well. Cells were incubated for another 1 h or until color developed. NBT was reduced by ROS to the dark blue formazan, which was dissolved in DMSO and its absorbance determined at 560 nm [22].

Dihydro-dichlorofluorescein diacetate assay

H_2DCF dye emits green fluorescence upon reaction with superoxide. AMs were treated as above and incubated in 10 µM of H_2DCF dye (Sigma-Aldrich). After 10-min incubation, fluorescence was measured using a fluorometer, using a 485 nm excitation and a 528 nm emission filter [22].

Inflammatory cytokine profiling

Cytokine concentrations of TNF-α, IL-6 and IL-1β were measured by ELISA kits (eBioscience Co, San Diego, CA) in samples of BALF or cell culture medium collected at the indicated time after bacterial infection. 100 μl aliquots of samples were added to the coated microtiter wells. The cytokine concentrations were determined with corresponding detection HRP-conjugated antibodies. The values were read at 450 nm [45].

MTT assay

Cells were treated as above, and incubated in 0.5 mg/ml MTT (Sigma-Aldrich) for 4 h. Reaction was stopped by stop solution and left at room temperature overnight for complete dissolution of formazan and absorbance at 560 nm was recorded using a multiscan plate reader to quantify the concentration of superoxide anion [46].

CFU assay

Phagocytosis and intracellular killing were assessed by CFU count assay as previously described [47]. Cells were challenged with bacteria at an MOI of 20:1 bacteria-cell ratio. The numbers of internalized and killed bacteria were assessed after 1 or 2 h of incubation. After 1 h, polymyxin B was added to the medium at 100 μg/ml for 30 min to kill extracellular bacteria. Cells were then lysed, and bacterial CFU were determined by plating samples to a LB dish. The phagocytosis efficiency was calculated on the basis of CFU data obtained 1 h after infection and was normalized to the control group [47].

Phagocytosis assay

MH-S cells were previously transfected with Rab5-RFP for 24 h [48], and then challenged with EGFP-expressing PA14 and mutants (green) at an MOI of 20:1 for 1 h. Cells were observed under an LSM 510 Meta Confocal Microscope (Carl Zeiss Micro Imaging, Thornwood, NY).

Immune response primer-profiling assay

RNA was isolated from MH-S cells after 2 h PA14 WT and ΔTCR mutant post infection. DNA-free RNA (100 ng) was used for the first strand of cDNA synthesis using a SuperScript III first-strand synthesis system (Fisher Scientific). PCR primers assay was performed using the iTag Universal SYBR Green Supermix (Bio-Rad) and gene-specific primers that attached on the bottom of the innate and immune response M384 predesigned 384-well panel (Bio-Rad), in a CFX Connect Real-time PCR Detection System (Bio-Rad). qRT-PCR array screening data were analyzed using PrimePCR analysis software (Bio-Rad).

Immunoblotting

Mouse monoclonal Abs against β-actin (sc-47778), TLR4 (sc-293072), NF-κB p50 (sc-166588), p-NF-κB p50 (sc-33022), Stat6 (sc-374021), and Jak2 (sc-390539), rabbit polyclonal Abs against TLR2 (sc-10739), and p-Jak2 (sc-21870), goat polyclonal Abs against TNF-α (sc-1349), IL-6 (sc-1265), IL-1β (sc-23460) and p-Stat6 (sc-11762) were obtained from Santa Cruz Biotechnology (Dallas, TX). The samples derived from cells and lung homogenates were lysed in RIPA buffer, separated by electrophoresis on 12% SDS-PAGE gels and transferred to nitrocellulose transfer membranes (GE Amersham Biosciences, Pittsburgh, PA). Proteins were detected by western blotting using primary Abs at a concen-

tration of 1/200 and incubated overnight. Labeling of the first Abs was detected using relevant secondary Abs conjugated to HRP (Santa Cruz Biotechnology), detected using ECL regents (Santa Cruz Biotechnology) and quantified by Quantity One software (Bio-Rad) [22].

Immunostaining

Cells were infected with indicated bacteria in an MOI of 20:1 bacteria-cell ratio for 0, 15, 30 and 60 min, and individually incubated with primary anti-p-NF-κB p65 (sc-166748) Ab or TLR4 Ab, and then the second FITC-conjugated antibodies as described [22]. 4,6-diamidino-2-phenylindole (DAPI, Sigma-Aldrich) was used to stain the nucleus.

RNA degradation assay

RNA degradation assays were performed as previously described [6]. Overnight cultures of bacteria were subcultured into 10 ml of M9 medium containing 0.2% cysteine and growth to $OD_{600\,nm}$ of about 1.0. Rifampicin was added to a final concentration of 500 μg/ml (Sigma-Aldrich), cultures were incubated at 37 °C with aeration, and aliquots were taken at the indicated time points for RNA isolation.

Phagosome purification

AMs infected with bacteria at indicated time point were collected and the phagosome purification was performed exactly following previously study [49, 50]. Total RNA of phagocytized bacteria was isolated from the phagosome and qPCR was performed. TLR4 levels in these phagosomes were also examined by immunoblotting.

Protein purification

Cultures of *E. coli* BL21 containing a plasmid expressing Csy1-4 complex were grown to an $OD_{600\,nm}$ of 0.5 and then induced with 1 mM IPTG (Sigma-Aldrich) for 16 h at 25 °C. Cultures of PA14 strains expressing WT Cas3 and its relevant mutants were grown at the same OD and then induced with 1 mM arabinose for 3 h at 37 °C. These recombinant proteins bear an N-terminal 6× His-tag, and were then affinity purified using Ni-NTA beads [51]. Purified proteins were then dialyzed into a buffer (20 mM HEPES, pH 7.5) for *in vitro* cleavage assay.

In vitro cleavage assay

The 40-bp single-strand *lasR* RNA substrate probes and crRNA were synthesized by Eurofins Genomics (Huntsville, AL). RNA probes were 5′ labeled with [γ-^{32}P]ATP using polynucleotide kinase (PNK, New England Biolabs) for 30 min at 37 °C. PNK was heat-denatured at 65 °C for 20 min, and excess ATP was removed using a G-25 spin column (GE Healthcare, Jupiter, FL).

All cleavage assays were performed in 1× reaction buffer (20 mM HEPES, pH 7.5, 100 mM KCl, 5 mM Mg₂Cl), following a previous study [41]. Csy1-4 complex was prebound to RNA substrate by incubating at 37 °C for 30 min. Samples were cooled on ice for 5 min before addition of ATP to a final concentration of 2 mM, indicated amount of crRNA and His-Cas3 or its mutants. The final concentration of RNA substrate was 1 nM, Csy1-4 complex was 1 μM. Samples were pretreated with 10 U protease K at 37 °C for 5 min to digest protein, and then resolved on denaturing gels containing 15% (v/v) 29:1 polyacrylamide, 8 M urea and 1× TBE.

Gels were dried and RNA fragments were visualized by exposure to X-ray film (Fisher Scientific) at −80 °C overnight.

EMSA assay

EMSA assay was performed using Molecular Probes EMSA kit (E33075). Proteins, [γ-^{32}P]ATP labeled RNA substrate and crRNA were mixed by incubating at 37 °C for 30 min. Samples were resolved on 2% agarose gel. Gels were dried and RNA fragments were visualized by exposure to X-ray film at −80 °C overnight.

Statistical analysis

Differences between the two groups were compared by using one-way ANOVA (Tukey's *post hoc*) using Graphpad Prism 5 software, whereas the mice survival rate was calculated using Kaplan-Meier curve [22].

Acknowledgments

Author Contributions

RL, GL, JJ and MW designed research and wrote the manuscript. RL, LF, MY, ST, XL and SH performed experiments. YW provided regents and suggestions.

Competing Financial Interests

The authors declare no competing financial interests.

References

1   Carte J, Christopher RT, Smith JT, *et al.* The three major types of CRISPR-Cas systems function independently in CRISPR RNA biogenesis in *Streptococcus thermophilus*. *Mol Microbiol* 2014; **93**:98-112.

2   Wiedenheft B, Sternberg SH, Doudna JA. RNA-guided genetic silencing systems in bacteria and archaea. *Nature* 2012; **482**:331-338.

3   Makarova KS, Wolf YI, Alkhnbashi OS, *et al.* An updated evolutionary classification of CRISPR-Cas systems. *Nat Rev Microbiol* 2015; **13**:722-736.

4   Shmakov S, Abudayyeh OO, Makarova KS, *et al.* Discovery and functional characterization of diverse class 2 CRISPR-Cas systems. *Mol Cell* 2015; **60**:385-397.

5   Westra ER, Buckling A, Fineran PC. CRISPR-Cas systems: beyond adaptive immunity. *Nat Rev Microbiol* 2014; **12**:317-326.

6   Sampson TR, Saroj SD, Llewellyn AC, Tzeng YL, Weiss DS. A CRISPR/Cas system mediates bacterial innate immune evasion and virulence. *Nature* 2013; **497**:254-257.

7   Louwen R, Horst-Kreft D, de Boer AG, *et al.* A novel link between *Campylobacter jejuni* bacteriophage defence, virulence and Guillain-Barre syndrome. *Eur J Clin Microbiol Infect Dis* 2013; **32**:207-226.

8   Aklujkar M, Lovley DR. Interference with histidyl-tRNA synthetase by a CRISPR spacer sequence as a factor in the evolution of *Pelobacter carbinolicus*. *BMC Evol Biol* 2010; **10**:230.

9   Jorth P, Whiteley M. An evolutionary link between natural transformation and CRISPR adaptive immunity. *MBio* 2012; **3**. pii:e00309-e00312.

10 Lyczak JB, Cannon CL, Pier GB. Establishment of *Pseudomonas aeruginosa* infection: lessons from a versatile opportunist. *Microbes Infect* 2000; **2**:1051-1060.

11 Rahme LG, Stevens EJ, Wolfort SF, Shao J, Tompkins RG, Ausubel FM. Common virulence factors for bacterial pathogenicity in plants and animals. *Science* 1995; **268**:1899-1902.

12 Tan MW, Rahme LG, Sternberg JA, Tompkins RG, Ausubel FM. *Pseudomonas aeruginosa* killing of *Caenorhabditis elegans* used to identify *P. aeruginosa* virulence factors. *Proc Natl Acad Sci USA* 1999; **96**:2408-2413.

13 Zegans ME, Wagner JC, Cady KC, Murphy DM, Hammond JH, O'Toole GA. Interaction between bacteriophage DMS3 and host CRISPR region inhibits group behaviors of *Pseudomonas aeruginosa*. *J Bacteriol* 2009; **191**:210-219.

14 Kooistra O, Bedoux G, Brecker L, *et al.* Structure of a highly phosphorylated lipopolysaccharide core in the Delta algC mutants derived from *Pseudomonas aeruginosa* wild-type strains PAO1 (serogroup O5) and PAC1R (serogroup O3). *Carbohydr Res* 2003; **338**:2667-2677.

15 Cady KC, O'Toole GA. Non-identity-mediated CRISPR-bacteriophage interaction mediated via the Csy and Cas3 proteins. *J Bacteriol* 2011; **193**:3433-3445.

16 Hauser AR. The type III secretion system of *Pseudomonas aeruginosa*: infection by injection. *Nat Rev Microbiol* 2009; **7**:654-665.

17 Sawa T, Shimizu M, Moriyama K, Wiener-Kronish JP. Association between *Pseudomonas aeruginosa* type III secretion, antibiotic resistance, and clinical outcome: a review. *Crit Care* 2014; **18**:668.

18 Zhao KL, Li Y, Yue BS, Wu M. Genes as early responders regulate quorum-sensing and control bacterial cooperation in *Pseudomonas aeruginosa*. *PLoS One* 2014; **9**:e101887.

19 Cass SD, Haas KA, Stoll B, *et al.* The role of Cas8 in type I CRISPR interference. *Biosci Rep* 2015; **35**. pii: e00197.

20 Bernstein JA, Khodursky AB, Lin PH, Lin-Chao S, Cohen SN. Global analysis of mRNA decay and abundance in *Escherichia coli* at single-gene resolution using two-color fluorescent DNA microarrays. *Proc Natl Acad Sci USA* 2002; **99**:9697-9702.

21 Rollins MF, Schuman JT, Paulus K, Bukhari HS, Wiedenheft B. Mechanism of foreign DNA recognition by a CRISPR RNA-guided surveillance complex from *Pseudomonas aeruginosa*. *Nucleic Acids Res* 2015; **43**:2216-2222.

22 Li R, Tan S, Yu M, Jundt MC, Zhang S, Wu M. Annexin A2 regulates autophagy in *Pseudomonas aeruginosa* infection through the Akt1-mTOR-ULK1/2 signaling pathway. *J Immu-

nol 2015; **195**:3901-3911.

23 Mei SH, Haitsma JJ, Dos Santos CC, *et al.* Mesenchymal stem cells reduce inflammation while enhancing bacterial clearance and improving survival in sepsis. *Am J Respir Crit Care Med* 2010; **182**:1047-1057.

24 Gao Y, Fang X, Tong Y, Liu Y, Zhang B. TLR4-mediated MyD88-dependent signaling pathway is activated by cerebral ischemia-reperfusion in cortex in mice. *Biomed Pharmacother* 2009; **63**:442-450.

25 Choi H, Choi H, Han J, *et al.* IL-4 inhibits the melanogenesis of normal human melanocytes through the JAK2-STAT6 signaling pathway. *J Invest Dermatol* 2013; **133**:528-536.

26 Zhou X, Li X, Ye Y, *et al.* MicroRNA-302b augments host defense to bacteria by regulating inflammatory responses via feedback to TLR/IRAK4 circuits. *Nat Commun* 2014; **5**:3619.

27 Kiratisin P, Tucker KD, Passador L. LasR, a transcriptional activator of *Pseudomonas aeruginosa* virulence genes, functions as a multimer. *J Bacteriol* 2002; **184**:4912-4919.

28 Staals RH, Zhu Y, Taylor DW, *et al.* RNA targeting by the type III-A CRISPR-Cas Csm complex of *Thermus thermophilus*. *Mol Cell* 2014; **56**:518-530.

29 Gunderson FF, Cianciotto NP. The CRISPR-associated gene cas2 of *Legionella pneumophila* is required for intracellular infection of amoebae. *MBio* 2013; **4**:e00074-e00013.

30 Luo ML, Mullis AS, Leenay RT, Beisel CL. Repurposing endogenous type I CRISPR-Cas systems for programmable gene repression. *Nucleic Acids Res* 2015; **43**:674-681.

31 Sinkunas T, Gasiunas G, Fremaux C, Barrangou R, Horvath P, Siksnys V. Cas3 is a single-stranded DNA nuclease and ATP-dependent helicase in the CRISPR/Cas immune system. *EMBO J* 2011; **30**:1335-1342.

32 Wiedenheft B, van Duijn E, Bultema JB, *et al.* RNA-guided complex from a bacterial immune system enhances target recognition through seed sequence interactions. *Proc Natl Acad Sci USA* 2011; **108**:10092-10097.

33 Wiedenheft B, Zhou K, Jinek M, Coyle SM, Ma W, Doudna JA. Structural basis for DNase activity of a conserved protein implicated in CRISPR-mediated genome defense. *Structure* 2009; **17**:904-912.

34 Weiss DS, Brotcke A, Henry T, Margolis JJ, Chan K, Monack DM. *In vivo* negative selection screen identifies genes required for *Francisella* virulence. *Proc Natl Acad Sci USA* 2007; **104**:6037-6042.

35 Buchanan PJ, Ernst RK, Elborn JS, Schock B. Role of CFTR, *Pseudomonas aeruginosa* and toll-like receptors in cystic fibrosis lung inflammation. *Biochem Soc Trans* 2009; **37**:863-867.

36 Epelman S, Stack D, Bell C, *et al.* Different domains of *Pseudomonas aeruginosa* exoenzyme S activate distinct TLRs. *J Immunol* 2004; **173**:2031-2040.

37 van der Oost J, Jore MM, Westra ER, Lundgren M, Brouns SJ. CRISPR-based adaptive and heritable immunity in prokaryotes. *Trends Biochem Sci* 2009; **34**:401-407.

38 Louwen R, Staals RH, Endtz HP, van Baarlen P, van der Oost J. The role of CRISPR-Cas systems in virulence of pathogenic bacteria. *Microbiol Mol Biol Rev* 2014; **78**:74-88.

39 Stern A, Keren L, Wurtzel O, Amitai G, Sorek R. Self-targeting by CRISPR: gene regulation or autoimmunity? *Trends Genet* 2010; **26**:335-340.

40 Fodah RA, Scott JB, Tam HH, *et al.* Correlation of *Klebsiella pneumoniae* comparative genetic analyses with virulence profiles in a murine respiratory disease model. *PLoS One* 2014; **9**:e107394.

41 Hochstrasser ML, Taylor DW, Bhat P, *et al.* CasA mediates Cas3-catalyzed target degradation during CRISPR RNA-guided interference. *Proc Natl Acad Sci USA* 2014; **111**:6618-6623.

42 Kannan S, Huang H, Seeger D, *et al.* Alveolar epithelial type II cells activate alveolar macrophages and mitigate *P. aeruginosa* infection. *PLoS One* 2009; **4**:e4891.

43 Li G, Fox J, 3rd, Liu Z, *et al.* Lyn mitigates mouse airway remodeling by downregulating the TGF-beta3 isoform in house dust mite models. *J Immunol* 2013; **191**:5359-5370.

44 Suzaki Y, Hamada K, Nomi T, *et al.* A small-molecule compound targeting CCR5 and CXCR3 prevents airway hyperresponsiveness and inflammation. *Eur Respir J* 2008; **31**:783-789.

45 Yan J, Liu X, Wang Y, *et al.* Enhancing the potency of HBV DNA vaccines using fusion genes of HBV-specific antigens and the N-terminal fragment of gp96. *J Gene Med* 2007; **9**:107-121.

46 Tan S, Gan C, Li R, *et al.* A novel chemosynthetic peptide with beta-sheet motif efficiently kills *Klebsiella pneumoniae* in a mouse model. *Int J Nanomedicine* 2015; **10**:1045-1059.

47 Yang K, Wu M, Li M, *et al.* miR-155 suppresses bacterial clearance in *Pseudomonas aeruginosa*-induced keratitis by targeting Rheb. *J Infect Dis* 2014; **210**:89-98.

48 Li X, He S, Zhou X, *et al.* Lyn delivers bacteria to lysosomes for eradication through TLR2-initiated autophagy related phagocytosis. *PLoS Pathog* 2016; **12**:e1005363.

49 Luhrmann A, Haas A. A method to purify bacteria-containing phagosomes from infected macrophages. *Methods Cell Sci* 2000; **22**:329-341.

50 Kannan S, Audet A, Huang H, Chen LJ, Wu M. Cholesterol-rich membrane rafts and Lyn are involved in phagocytosis during *Pseudomonas aeruginosa* infection. *J Immunol* 2008; **180**:2396-2408.

51 Bondy-Denomy J, Garcia B, Strum S, *et al.* Multiple mechanisms for CRISPR-Cas inhibition by anti-CRISPR proteins. *Nature* 2015; **526**:136-139.

(**Supplementary information** is linked to the online version of the paper on the *Cell Research* website.)